Dalton Transactions

PAPER

View Article Online
View Journal | View Issue

Cite this: *Dalton Trans.*, 2016, **45**, 10672

Synthesis and reactivity of Li and $TaMe_3$ complexes supported by *N*,*N*′-bis(2,6-diisopropylphenyl)-*o*-phenylenediamido ligands†

Trevor Janes, Maotong Xu and Datong Song*

Received 14th May 2016,
Accepted 1st June 2016

DOI: 10.1039/c6dt01908k

www.rsc.org/dalton

The dilithium complex of *N*,*N*′-bis(2,6-diisopropylphenyl)-*o*-phenylenediamide, $[Li_2L(thf)_3]$, reacts with $TaMe_3Cl_2$ in THF/Et_2O to yield $[Li(Et_2O)(thf)LTaMe_3Cl]$ in which the phenylene backbone of $\mathbf{L}^{2-}$ is bound η^4 to the Ta centre. This dinuclear species reacts with MeLi to yield the tetramethyltantalum complex $[Li(Et_2O)(thf)LTaMe_4]$. Double deprotonation of *N*,*N*′-bis(2,6-diisopropylphenyl)(4,5-dimethyl)-*o*-phenylenediamine (H_2L') in Et_2O yielded the dilithium complex $[Li_2L'(OEt_2)_2]$. The two additional methyl groups on L'^{2-} change the observed reactivity towards $TaMe_3Cl_2$: rather than bridging between Ta and Li, ligand oxidation occurs to afford mononuclear $[LiL'(OEt_2)]$. This monolithium radical species, which was characterized by EPR spectroscopy, can also be synthesized using the more conventional oxidant $AgBF_4$. Double deprotonation of H_2L with KCH_2Ph in toluene followed by reaction with $TaMe_3Cl_2$ furnished $[TaLMe_3]$. Preliminary reactivity studies show $[TaLMe_3]$ reacts with unsaturated substrates *N*,*N*′-dicyclohexylcarbodiimide and mesityl azide to undergo migratory insertion into one of the Ta–C bonds: the corresponding amidinate and triazenido ligands are generated. When subjected to UV irradiation, $[TaLMe_3]$ undergoes reduction accompanied by loss of a methyl group to yield the dimeric species $[TaLMe_2]_2$.

Introduction

Since Juvinall's 1964 preparation of the first tantalum methyl complex, $TaMe_3Cl_2$,[1] organometallic chemists have been interested in the synthesis and reactivity of Ta–Me species. Members of the research community have continued to design and invent Ta–Me complexes supported by diverse ancillary ligand sets which have facilitated fascinating reactivity. Schrock's syntheses of the homoleptic $TaMe_5$ [2] which violently decomposes *via* alpha abstraction,[3] and the first transition metal methylidene complex, $[Cp_2Ta(CH_3)(CH_2)]$[4] are seminal examples. Fryzuk and coworkers discovered that a $TaMe_3$ fragment chelated by their $(PhP(CH_2SiMe_2NPh)_2)^{2-}$ ligand undergoes hydrogenolysis to yield a dinuclear tetrahydride species,[5] a lynchpin in the field of N_2 activation. More recently, phosphoramidate ligands have been used to sponsor $TaMe_3Cl$ precatalysts for room temperature hydroaminoalkylation of olefins.[6] Ta methyls have also been grafted onto silica supports for use as well-defined heterogeneous precatalysts for ethylene trimerization[7] and alkane metathesis.[8]

Multiple reports have emerged on the synthesis and reactivity of tantalum complexes of diamido ligands with pendant neutral donor functionalities. Fryzuk's work with diamidophosphine[5,9–19] and diamidodiphosphine[20–22] ligand families is very well-represented. Other prominent examples include Heyduk's redox active NNN-pincer ligand,[23–25] diamidoamines[26–31] and diamidoaminopyridines.[32,33] Tridentate diamido ligands in which the additional donor is a pyridine,[27,34,35] carbene,[36] arsine,[37] and thioether[38] are also known. Compared to this abundance of examples of Ta complexes of decorated diamido ligands, simple diamido ligands have not been as well-studied. Tantalum complexes of ligands based on 1,8-diamidonaphthalene,[39–41] 1,3-diamidopropane,[42,43] 1,4-diaza-1,3-butadiene,[44–49] and *o*-phenylenediamide (opda) are known. Of the opda complexes, most employ *N*,*N*′-disilyl groups,[41,50–53] with one report on neopentyl groups.[54] To our knowledge, tantalum complexes of *N*,*N*′-diaryl substituted opda ligands are heretofore unknown.

We have been investigating the coordination chemistry of *N*,*N*′-bis(2,6-diisopropylphenyl)-*o*-phenylenediamide,[55] $\mathbf{L}^{2-}$, and sought to prepare Ta complexes of this simple bulky ligand, which may engender new and complementary reactivity to related ligands mentioned above. Herein we report our efforts to coordinate dipp-substituted opda ligands to Ta.

---

*Davenport Chemical Research Laboratories, Department of Chemistry, University of Toronto, 80 St. George Street, Toronto, Ontario M5S 3H6, Canada.
E-mail: dsong@chem.utoronto.ca*

† Electronic supplementary information (ESI) available: NMR spectra and X-ray crystallographic experimental details. CCDC 1479767–1479775. For ESI and crystallographic data in CIF or other electronic format see DOI: 10.1039/c6dt01908k

Results and discussion

Synthesis and structures of heterodinuclear compounds 2 and 3(solvent)$_n$

Addition of an Et_2O solution of $TaMe_3Cl_2$ to a THF solution of $Li_2L(thf)_3$ at −70 °C caused the reaction mixture to gradually turn orange as compound **2** formed (Scheme 1). After removal of LiCl, The ^7Li NMR spectrum of **2** still featured a singlet at 2.03 ppm, distinct from the ^7Li resonance of **1** (2.62 ppm), which indicated incomplete transfer of the diamido ligand from Li. The ^1H NMR resonances of the two sets of equivalent *o*-phenylene protons shifted upfield from 6.57 and 6.33 ppm in starting material **1** to 5.64 and 4.02 ppm in product **2**, which is consistent with coordination of the phenylene backbone to Ta. The nine Ta-bound methyl protons resonate as a broad singlet at 0.91 ppm at room temperature. Single crystals were grown by cooling an Et_2O solution of **2** to −25 °C. X-ray crystallography revealed the heterodinuclear nature of **2** (Fig. 1). The two opda nitrogen donor atoms of $\mathbf{L}^{2-}$ chelate the Li atom; its distorted tetrahedral coordination geometry is completed by the oxygen of one disordered Et_2O molecule and the oxygen of one ligand modelled as a 50 : 50 mixture of THF/Et_2O. $\mathbf{L}^{2-}$ forms a bridge to Ta *via* an η^4 interaction with its phenylene backbone. The coordination geometry at Ta is akin to a distorted trigonal bipyramid in which one apical ligand has been replaced with a π-bound diene. Cl^- occupies the other apical position and three equatorial methyl groups complete the coordination sphere of Ta. The solid state structure suggests two different environments for Ta–Me protons, but cooling a toluene-d_8 solution of **2** to −80 °C did not resolve the ^1H NMR signal of the methyl groups, which suggests conformational fluxionality with a low barrier.

The apical chloride ligand of **2** can be replaced by a methyl group by treatment with MeLi. Addition of MeLi in Et_2O to a solution of **2** at −35 °C yielded the tetramethyltantalum complex $[Li(Et_2O)(thf)LTaMe_4]$, **3**$(Et_2O)(thf)$. The transformation from **2** to **3**$(Et_2O)(thf)$ causes a subtle change in the ^7Li NMR spectrum: the singlet shifts from 2.03 ppm to 2.26 ppm. Similarly, subtle peak shifts are observed in the ^1H NMR spectrum of **3**$(Et_2O)(thf)$. Distinct from **2**, the Ta–Me proton resonance at 0.89 ppm is even more dramatically broadened at room temperature. Single crystals for X-ray analysis were obtained by cooling a pentane solution of **3**$(Et_2O)(thf)$ to −25 °C (Fig. 1). The solid state data confirmed the replacement of the chloride by a methyl ligand and that the η^4 butadiene-type interaction is conserved in the methylation. The solid state structure contains two THF ligands on Li rather than one Et_2O and one THF, which is expected based on ^1H NMR data. This phenomenon can be explained by ligand exchange on Li and preferential crystallization of **3**$(thf)_2$. When **3**$(Et_2O)(thf)$ is recrystallized from a mixture of pentane and Et_2O, resonances from coordinated THF disappear, and only one Et_2O ligand is present. This species, **3**(Et_2O), possesses a simpler alkyl region of the ^1H NMR spectrum; upon cooling a toluene-d_8 solution to −80 °C, the broad Ta–Me peak splits into three distinct singlets (see ESI†), consistent with the solid state structure. Two of the peaks integrate to three protons each (2.35 and 1.00 ppm) for the two methyl ligands sitting on the mirror plane that bisects the $\mathbf{L}^{2-}$ and the third peak integrates to six protons (0.42 ppm) for the two methyl ligands that are related by this mirror plane.

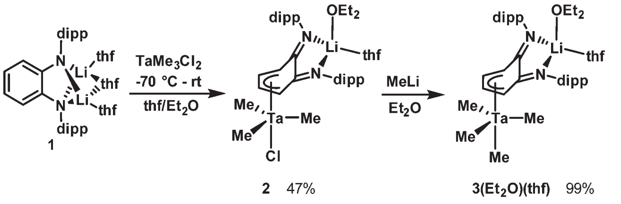

Scheme 1 Synthesis of Ta–Li heterodinuclear complexes **2** and **3**$(Et_2O)(thf)$.

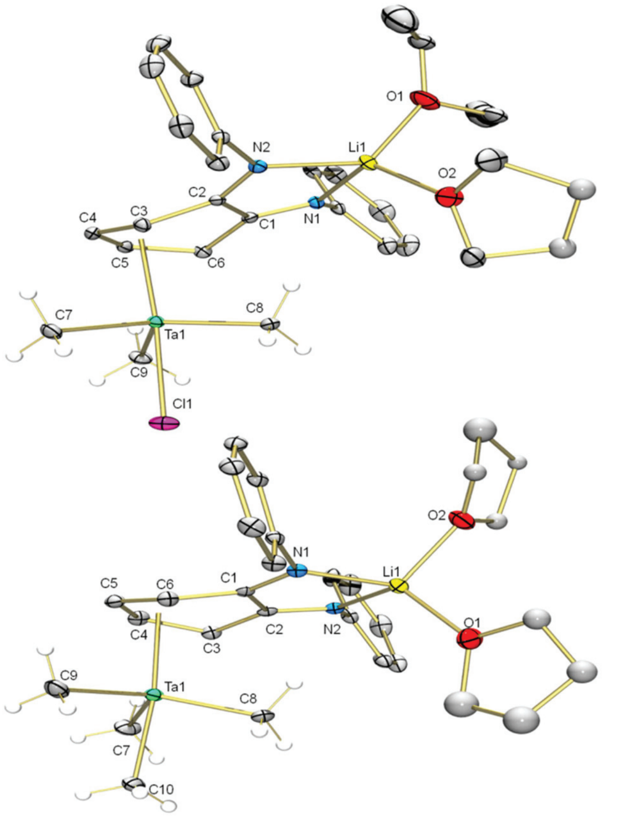

Fig. 1 Molecular structures of **2** (top) and **3**$(thf)_2$ (bottom). Non-hydrogen atoms are shown as 30% probability ellipsoids except for the disordered portion of Li-coordinated thf. Ta–Me H atoms are shown as spheres of arbitrary radius, the rest of the H-atoms along with the isopropyl groups on L are omitted for clarity. Selected bond angles (°) for **2**: N1–Li1–N2 82.1(2), C7–Ta1–C8 118.7(1), C8–Ta1–C9 120.2(1), C7–Ta1–C9 111.8(1), Cl1–Ta1–C7 80.25(9), Cl1–Ta1–C8 80.01(9), Cl1–Ta1–C9 78.96(9). Selected bond angles (°) for **3**$(thf)_2$: N1–Li1–N2 82.6(3), C7–Ta1–C8 116.5(2), C8–Ta1–C9 118.3(2), C7–Ta1–C9 114.7(2). C7–Ta1–C10 78.1(2), C8–Ta1–C10 80.6(2), C9–Ta1–C10 78.3(2).

The solid state molecular structures of **2** and **3**$(thf)_2$ are very similar. In both, the lithium atom is chelated by the two nitrogen donor atoms of the $\mathbf{L}^{2-}$. The $C_{phenylene}$–N bond lengths (1.295(4) Å in **2** and 1.306(5) and 1.307(5) Å in **3**(thf)$_2$) are significantly shortened compared to the dilithium complex **1** ($C_{phenylene}$–N bond lengths of 1.396(2) and 1.395(2) Å).[55] This compression of C–N bonds suggests the diamido ligand in **1** has become a diimine ligand in **2** and **3**(thf)$_2$. The tantalum atom in **2** and **3**(thf)$_2$ is bound η^4- to the *o*-phenylene ring of the opda ligand in a butadiene-type interaction. In these complexes, the η^4-C_6 ring is folded along the C3–C6 vector at angles of 31° and 25°, respectively which are very similar to the corresponding angle in the previously reported trimetallic $[(Li(thf)_2L)_2MoCl_2]$ (30°).[55] On the continuum between the Chatt-Dewar diene (L_2) and metallocyclopentene (LX_2) extremes,[56] we formulated this $MoLi_2$ species as more of an L_2 butadiene-type complex. However, the metric parameters of the η^4 ligand used to make this assignment are different from Ta complexes **2** and **3**(thf)$_2$. The Δd parameter (where Δd = avg. M–C_{outer} bond length – avg. M–C_{inner} bond length; C_{outer} refers to C3 and C6 and C_{inner} refers to C4 and C5) is 0.034(3) Å for **2** and 0.060(4) Å for **3**(thf)$_2$, compared to 0.142(6) Å in the $MoLi_2$ species. In the $MoLi_2$ species, the C_{inner}–C_{inner} and avg. C_{inner}–C_{outer} bonds are statistically similar, but in **2** and **3**(thf)$_2$, the C_{inner}–C_{inner} bonds are 1.377(4) and 1.368(6) Å, respectively. These bonds are significantly shorter than the avg. C_{inner}–C_{outer} in **2** and **3**(thf)$_2$, which are 1.431(4) and 1.427(4) Å. **2** and **3**(thf)$_2$ more closely resemble the metallocyclopentene resonance form, which is consistent with the greater electropositivity of Ta relative to Mo. Taken together, the metric parameters of both **2** and **3**(thf)$_2$ suggest contribution of $\mathbf{L}^{2-}$ resonance form B (Chart 1) is significant (Table 1).

Coordination chemistry of L′

In hopes of disfavouring the phenylene carbons relative to the diamido nitrogens as coordination site for Ta we increased the steric bulk at the phenylene backbone. According to the method of Wenderski *et al.*,[57] we synthesized the doubly methylated diamine proligand $\mathbf{H_2L'}$. Double deprotonation was achieved by addition of two equivalents of *n*-BuLi to a −70 °C diethylether solution of **4** (Scheme 2). After removal of volatiles and precipitation with cold pentane, $[Li_2L'(Et_2O)_2]$, **5**, was isolated as a white powder. In the ^{1}H NMR spectrum of **5** in C_6D_6, the N–H resonance present in the starting material is absent, replaced by a quartet at 2.92 ppm and a triplet at 0.74 ppm corresponding to the ethyl groups on two coordinated Et_2O molecules. In the ^{7}Li NMR spectrum, one signal is observed at 0.77 ppm which indicates that the two Li atoms are equivalent in solution. Single crystals for X-ray were obtained by cooling a pentane/Et_2O solution to −25 °C (see ESI†).

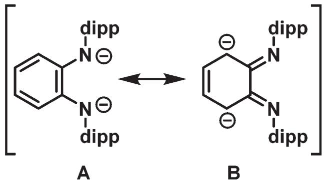

Chart 1 Two resonance forms for $\mathbf{L}^{2-}$.

Table 1 Selected bond lengths for **2** and **3**(thf)$_2$

Bond	Length in **2** (Å)	Length in **3**(thf)$_2$ (Å)	Bond	Length in **2** (Å)	Length in **3**(thf)$_2$ (Å)
Ta1–C3	2.443(3)	2.480(4)	C2–C3	1.451(5)	1.428(6)
Ta1–C4	2.401(4)	2.422(4)	C3–C4	1.426(5)	1.430(5)
Ta1–C5	2.400(3)	2.419(4)	C4–C5	1.377(4)	1.368(6)
Ta1–C6	2.425(3)	2.481(4)	C5–C6	1.436(5)	1.424(6)
Ta1–C7	2.205(3)	2.199(4)	C1–C6	1.443(4)	1.425(5)
Ta1–C8	2.209(4)	2.172(4)	C1–N1	1.295(4)	1.306(5)
Ta1–C9	2.218(3)	2.218(6)	C2–N2	1.295(4)	1.307(5)
Ta1–Cl1	2.428(1)		N1–Li1	2.058(5)	2.043(8)
Ta1–C10		2.241(5)	N2–Li1	2.076(6)	2.055(7)
C1–C2	1.488(4)	1.483(6)			

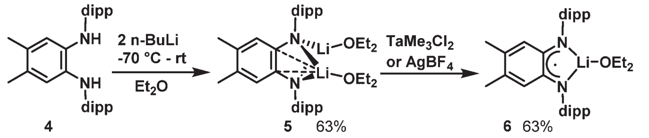

Scheme 2 Syntheses of Li complexes **5** and **6**.

Reaction of dilithium compound **5** with $TaMe_3Cl_2$ causes the solution to darken in colour. After replacing the solvent with pentane and removing insoluble material by filtration, dark green single crystals of **6** grew from the cooled concentrated pentane extract (see ESI† for X-ray structure and EPR spectrum). Unexpectedly, $TaMe_3Cl_2$ acted as an oxidant towards the dilithium species **5** and the $\mathbf{L}'^{2-}$ complex has lost an electron and a Li ion to become a monolithium diiminosemiquinonate complex. Efforts to structurally characterize the Ta-containing species generated in this reaction have so far not been fruitful. Notably, **6** can also be prepared by oxidation of **5** with a source of Ag^+ (see Experimental section).

Synthesis of [TaLMe$_3$], 8

In further efforts to synthesize an NN chelate complex of Ta with dipp-substituted opda ligands we employed dilithium salts of $\mathbf{L}^{2-}$ free of coordinated Et_2O/THF ligands; we also attempted protonolysis by reacting H_2L with $TaMe_3Cl_2$ or $Ta(NMe_2)_5$, but none of these attempts succeeded. However, the generation of the dipotassium salt of $\mathbf{L}^{2-}$ by double deprotonation of $\mathbf{H_2L}$ with benzylpotassium (for its molecular structure with complexed 1,2-dimethoxyethane ligands see ESI†) followed by reaction with $TaMe_3Cl_2$ in toluene yielded the desired $[TaLMe_3]$, **8** (Scheme 3). In its ^{1}H NMR spectrum in C_6D_6 at room temperature, the three methyl ligands resonate as a single peak at 1.03 ppm. Cooling a toluene-d_8 solution to −80 °C did not lead to any decoalescence of this signal. X-ray quality single crystals were grown by cooling a saturated pentane solution to −25 °C. The molecular structure of **8** (Fig. 2) reveals $\mathbf{L}^{2-}$ chelating a five-coordinate Ta centre, which is bound to three terminal methyl ligands. Ta occupies a distorted square pyramidal geometry, with N1, N2, C7 and C8 forming the square base and C9 in the apical position. The

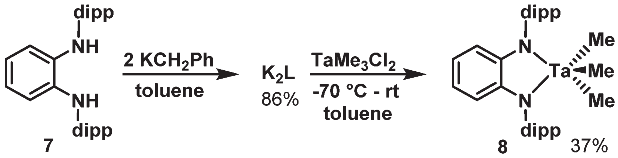

Scheme 3 Synthesis of [$TaLMe_3$].

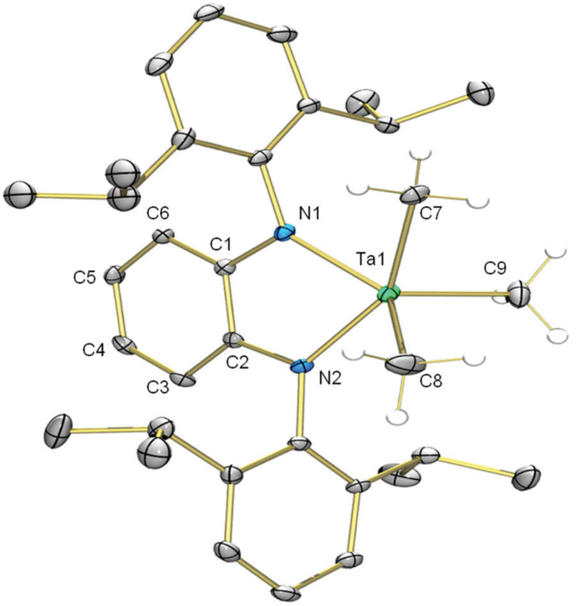

Fig. 2 Molecular structure of [$TaLMe_3$], **8**. Non-hydrogen atoms are shown as 30% probability ellipsoids. Hydrogen atoms on Ta–Me groups are shown as spheres of arbitrary radius, and the rest of the H-atoms are omitted for clarity. Only one orientation of disordered isopropyl group is shown. Selected bond lengths (Å) and angles (°) for **8**: Ta1–C7 2.177(4), Ta1–C8 2.137(6), Ta1–C9 2.137(5), Ta1–N1 2.055(3), Ta1–N2 2.052(3), C1–C2 1.390(6), C2–C3 1.391(6), C3–C4 1.390(6), C4–C5 1.394(6), 1.387(6), C6–C1 1.400(6), C1–N1 1.413(5), C2–N2 1.413(5), N1–Ta1–N2 75.5(1), N1–Ta1–C9 112.3(2), N1–Ta1-C8 138.6(2), N2–Ta1–C7 152.9(1), N2–Ta1–C8 92.3(2), N2–Ta1–C9 105.3(2), C7–Ta1-C8 89.9(2), C7–Ta1–C9 99.5(2), C8–Ta1–C9 109.1(2).

diamido ligand binds Ta with Ta1–N1 and Ta1–N2 bond lengths of 2.055(3) and 2.052(3) Å, respectively. The diamido's N1–Ta1–N2 bite angle is 75.5(1)°, and the five-membered TaN_2C_2 chelate ring is essentially planar such that the electron pairs on the nitrogen atoms are oriented with correct symmetry to engage in π-bonding with Ta. All *o*-phenylene C–C bond lengths are statistically similar and both $C_{phenylene}$–N bond lengths are 1.413(5) Å, statistically similar to the $C_{phenylene}$–N bond lengths in **5**. These data suggest the potentially redox-active $\mathbf{L}^{2-}$ maintains its dianionic charge, with resonance form A in Chart 1 as the major contributor.

8 could also be generated by thermal loss of LiCl from **2**. Heating a solution of **2** in C_6D_6 at 80 °C for 3 h caused consumption of **2**; analysis of the ^1H NMR spectrum indicated formation of **8** in a mixture that also contained [$TaClLMe_2$] and **3** (respective ratio of 1 : 1.5 : 2). The formation of [$TaClLMe_2$] can be explained by the exchange of Me and Cl ligands between Ta centres, which is well documented in the literature.[58]

Reactivity of [$TaLMe_3$]

Insertion of carbodiimides into Ta–C_{Me} bonds has been known since Wilkins' report in 1974.[59] To test the ability of **L** to sponsor this reaction we subjected **8** to one equivalent of *N*,*N*′-dicyclohexylcarbodiimide (DCC) (Scheme 4); the reaction mixture turned cherry red as insertion of DCC into one of the Ta–C bonds occurred. Diagnostic features of the ^{13}C NMR spectrum of **9** are the amidinate NCN and CH_3 resonances at 180.18 ppm and 15.12 ppm, respectively. In the ^1H NMR spectrum, the amidinate and Ta-bound CH_3 protons resonate as singlets integrating to three and six protons at 1.63 ppm and 1.03 ppm, respectively. All other alkyl protons give rise to broadened, overlapped resonances. X-ray analysis of single crystals revealed the molecular structure of **9** (Fig. 3) which includes a newly formed amidinate ligand. The geometry at Ta can be described as distorted trigonal prismatic, with N1–N2–C8 forming one triangular face and N3–N4–C7 forming the other. The amidinate coordination bond lengths are significantly different: N4–Ta1 (2.136(4) Å) is shorter than N3–Ta1 (2.221(4) Å). Its C–N bonds (1.325(6) and 1.344(7) Å) are equal within experimental error. The amidinate ligand chelates the tantalum centre with an N3–Ta1–N4 bite angle of 60.4(1)°, and the four-membered CN_2Ta ring is planar. Unlike **8**, the five-membered C_2N_2Ta ring exists in an envelope conformation, with the Ta atom out of plane. The dihedral angle between the *o*-phenylene plane and the plane defined by N1–Ta1–N2 is *ca.* 25°.

When mesityl azide was added to a solution of **8**, yellow precipitate formed. The ^1H NMR resonance associated with the Ta–bound Me groups shifted upfield to 0.67 ppm and its integration was reduced from nine to six protons, which indicated that the azide had reacted with one of the Me ligands on tantalum. Aside from resonances associated with the new mesityl group, an additional methyl singlet appeared at 2.53 ppm. X-ray crystallography on single crystals of **10** revealed that insertion of the azide into the tantalum–carbon bond had taken place, forming a κ^2-N_2 triazenido ligand. The Ta centre adopts a distorted trigonal bipyramidal geometry, with the equatorial positions occupied by the two Ta–Me groups and N1 of $\mathbf{L}^{2-}$. N2 of $\mathbf{L}^{2-}$ and the κ^2-N_2 interaction occupy the axial positions. The N3–Ta1 bond (2.049(2) Å) is significantly

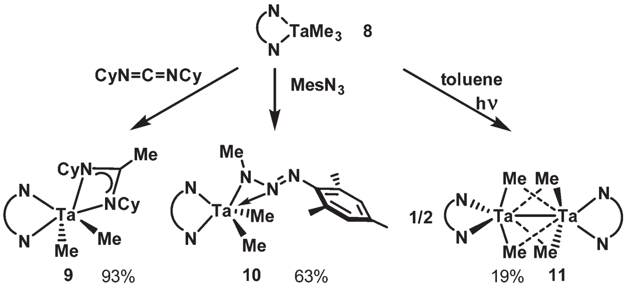

Scheme 4 Reactivity of [$TaLMe_3$]: synthesis of **9**, **10**, and **11**.

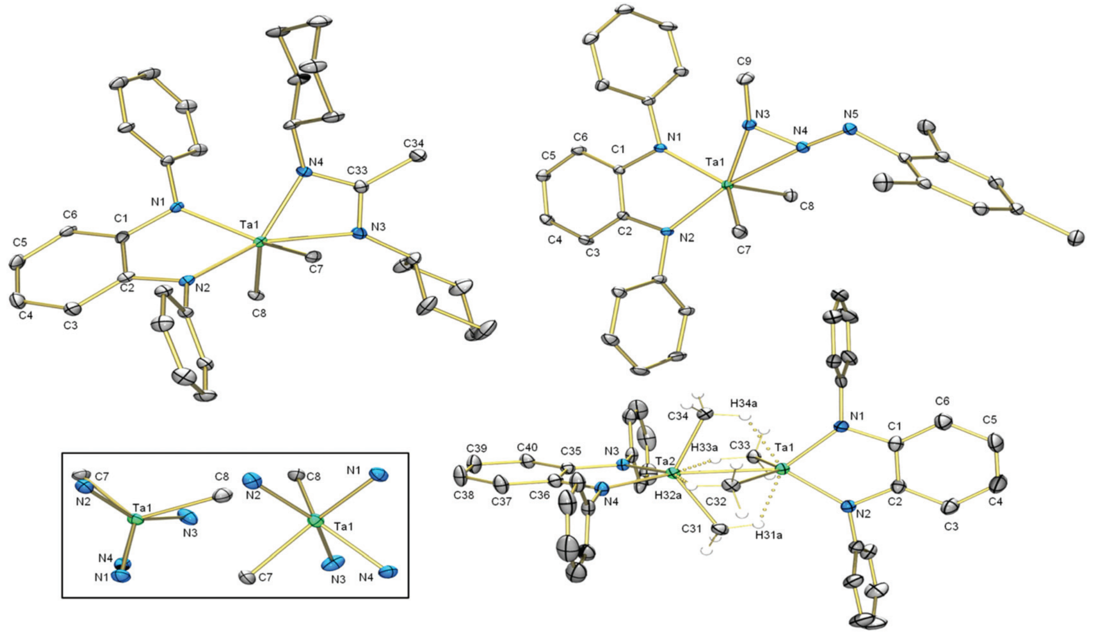

Fig. 3 Molecular structures of **9** (top left), **10** (top right), and **11** (bottom right). Inset: Two views of the coordination sphere of **9**. Non-hydrogen atoms are shown as 30% probability ellipsoids. Hydrogen atoms on the Ta–Me groups of **11** are shown as spheres of arbitrary radius. The rest of the H-atoms and isopropyl groups on L are omitted for clarity. Selected bond lengths (Å) and angles (°) for **9**: Ta1–N3 2.221(4), Ta1–N4 2.136(4), C33–N3 1.325(6), C33–N4 1.344(7). N1–Ta1–N2 77.0(1), N1–Ta1–N3 129.5(2), N1–Ta1–N4 86.3(1), N1–Ta1–C7 136.3(2), N1–Ta1–C8 95.1(2), N2–Ta1–N3 152.4(2), N2–Ta1–N4 139.5(1), N2–Ta1–C7 79.9(2), N2–Ta1–C8 88.2(2), N3–Ta1–N4 60.4(1), N3–Ta1–C7 82.9(2), N3–Ta1–C8 82.2(2), N4–Ta1–C7 87.8(2), N4–Ta1–C8 130.3(2), C7–Ta1–C8 120.9(2). Selected bond lengths (Å) and angles (°) for **10**: Ta1–N3 2.049(2), Ta1–N4 2.221(2) N4–N5 1.263(3), Ta1–N3–N4 79.0(1), N1–Ta1–N2 75.57(8), N1–Ta1–N3 83.71(8), N1–Ta1–N4 117.33(8), N1–Ta1–C7 137.13(8), N1–Ta1–C8 106.60(8), N2–Ta1–N3 152.50(8), N2–Ta1–N4 166.45(7), N2–Ta1–C7 85.78(8), N2–Ta1–C8 95.11(8), N3–Ta1–N4 36.16(8), N3–Ta1–C7 97.76(9), N3–Ta1–C8 108.17(9), N4–Ta1–C7 81.63(8), N4–Ta1–C8 85.35(8), C7–Ta1–C8 113.34(9). Selected distances (Å) and angles (°) for **11**: Ta1–Ta2 2.7120(5) Ta1–H31a 1.99, Ta1–H34a 1.98, Ta1–C31 2.618(5), Ta1–C34 2.607(4), Ta2–H32a 2.00, Ta2–H33a 1.99, Ta2–C32 2.627(4), Ta2–C33 2.614(4), Ta2–N3 2.033(3), Ta2–N4 2.032(3), C35–N3 1.425(5), C36–N4 1.432(5), C35–36 1.409(6), C36–C37 1.376(6), C37–C38 1.379(7), C38–C39 1.371(6), C39–C40 1.394(6), C35–C40 1.385(6). N2–Ta1–N1 82.1(1), N1–Ta1–H34a 72.2, H34a–Ta1–Ta2 67.5, Ta2–Ta1–H31a 67.7, H31a–Ta1–N2 70.6, C33–Ta1–C32 127.1(2), N3–Ta2–N4 81.9(1), N4–Ta2–H32a 71.8, H32a–Ta2–Ta1 67.7, Ta1–Ta2–H33a, H33a––Ta2–N3 71.3, C31–Ta2–C34 126.7(2).

shorter than the N4–Ta1 bond (2.221(2) Å) and the N4–N5 bond (1.263(3) Å) is shorter than the N4–N3 bond (1.335(3) Å), which informs our formulation of **10** shown in Scheme 4. The sum of the angles at N3 (359.8(3)°) indicates its planarity such that its lone pair be oriented perpendicular to this plane with correct symmetry to engage in π-bonding with Ta. The plane of the *o*-phenylene ring and the plane defined by the three nitrogen atoms of the triazenido ligand meet with a dihedral angle of 32°. For the diamido moiety, intraligand metric parameters are the same as in **8**; the diamido behaves as a spectator ligand during the transformation from **8** to **10**.

The reactivity most relevant to this transformation is the single and double insertion of aryl azides into the Ta–C bonds of [(ONO)TaMe2] (ONO = bis(phenoxy)amide ligand) to form mono and bis triazenido complexes.[60] Distinct from these compounds, the triazenido ligands in **10** are $\kappa^2N^{1,2}$-bound to Ta. Although this binding mode is well known for f-elements,[61–65] to our knowledge this is the first crystallographically characterized example of a triazenido ligand $\kappa^2N^{1,2}$-bound to Ta.

When a toluene solution of **8** was subjected to UV light, the colour of the solution darkened. In the ^{1}H NMR spectrum in C_6D_6, the Ta–Me resonance shifted upfield from 1.03 to 0.08 ppm, and there are six Ta–Me protons per diamido ligand, indicating loss of one of the Ta–Me groups. In the ^{13}C NMR spectrum the carbon peak attributable to the Ta–Me groups shifted from 83.50 ($^1J_{C-H}$ = 118 Hz) to 49.22 ppm ($^1J_{C-H}$ = 116 Hz). Single crystals of **11** were obtained from cold pentane; the molecular structure (Fig. 3, bottom) revealed a dimeric formally Ta(IV) species possessing a Ta–Ta bond length of 2.7120(5) Å. This bond is intermediate between the Ta–Ta bonds found in $(\mu\text{-H})_4$ ditantalum complexes of diamidophosphine (2.830(4) Å)[9] and diamidodiphosphine (2.6165(5) Å)[21] complexes. Each Ta centre is bound to two methyl groups, and each methyl group makes a close contact with its neighbouring Ta centre two bonds away; these distances range from 2.607(4) Å for Ta1–C34 to 2.627(4) Å for Ta1–C32. Although the methyl hydrogens were not located on the Fourier difference map, the proximity of the methyl carbons to both Ta centres and the marked shift of the methyl protons to high field in the ^{1}H NMR spectrum lend support for the presence of agostic interactions between one methyl C–H bond and its opposite Ta centre. Taking these interactions into account, the geometry at each seven-coordinate Ta centre is best understood as distorted pentagonal bipyramidal. On each Ta centre, $\mathbf{L}^{2-}$, the other Ta atom, and two agostic interactions reside in equatorial positions (sum of the bond angles: 360.1 at Ta1 and at Ta2). The two-centre two-electron bound methyl carbons occupy axial positions. This reactivity of $[TaLMe_3]$, which contains a simple diamido ligand, is distinct from that of Fryzuk's $[(P_2N_2)TaMe_3]$ (P_2N_2 = diamidodiphosphine ligand), which undergoes loss of methane to generate a monomeric methyl methylidene complex.[20] The authors proposed that the first step of the reaction was the photoinduced Ta–C bond homolysis, generating a methyl radical. Presumably the transformation of **8** to **11** could share the same initial step, where the methyl radical could be scavenged by toluene solvent and the resulting $[TaLMe_2]$ species dimerizes to form **11**.

Conclusion

Attempts were made to install simple, bulky opda ligands on Ta *via* salt metathesis with $TaMe_3Cl_2$. Use of dilithium complex **1** led to the isolation of heterodinuclear **2** in which the NN chelate site of the diamide ligand was occupied by Li^+, and the *o*-phenylene backbone was engaged in a η^4-interaction with Ta. This species underwent clean methylation with MeLi to generate tetramethyl species **3**(Et_2O)(thf) in which heterodinuclearity is preserved. A new dilithium complex with increased steric bulk at the *o*-phenylene backbone (**5**) was synthesized. When reacted with $TaMe_3Cl_2$ it underwent oxidation to open-shell monolithium complex **6**, which could be synthesized in higher yield and purity using $AgBF_4$. By using a dipotassium derivative of $\mathbf{L}^{2-}$, the desired trimethyltantalum complex (**8**) could be synthesized. Preliminary reactivity studies show **8** undergoes insertion reactions with DCC and $MesN_3$ to generate compounds **9** and **10**. In **10** the newly formed triazenido ligand is bound $\kappa^2N^{1,2}$, a bonding mode which is unusual for Ta. Irradiation of a toluene solution of **8** leads to isolation of dimeric Ta(IV) species **11**, which illustrates the complementary reactivity engendered by the simple bulky opda ligand. Our initial attempts to generate isolable Ta–H species *via* hydrogenolysis of **8** have not succeeded, but investigation of the reactivity of this and other *o*-phenylenediamido Ta complexes towards H_2 is ongoing in our laboratory.

Experimental section

General considerations

Compounds **1**,[55] **4**, **7**,[57] $TaMe_3Cl_2$,[4] KCH_2Ph,[66] and $MesN_3$[67] were prepared from literature methods. Methyl lithium (1.6 M in ether), *n*-butyl lithium (1.6 M in hexanes), $AgBF_4$, and N,N′-dicyclohexylcarbodiimide were purchased from commercial sources. All operations were performed using Schlenk techniques under dinitrogen or in a dinitrogen-filled glovebox. All glassware was either flame-dried or dried overnight in a 180 °C oven prior to use except for NMR tubes which were dried overnight in a 60 °C oven. THF, Et_2O, toluene, and C_6D_6 were distilled from Na/benzophenone under N_2. Pentane, hexanes, and toluene-d_8 were distilled from sodium under dinitrogen. All solvents were then stored over 3 Å molecular sieves prior to use. ^1H, ^{31}P, ^{13}C, and ^{11}B NMR spectra were recorded on a Varian 400 MHz, Agilent DD2 500 MHz, or Agilent DD2 600 MHz spectrometer. Electron paramagnetic resonance (EPR) spectra were obtained at 298 K in thf solution using a Bruker ECS-EMX X-band EPR spectrometer equipped with an ER4119HS cavity. Simulation was carried out using PEST WinSIM Software. All chemical shifts are reported in ppm relative the residual protio-solvent peaks ^7Li NMR is referenced externally using 9.7 M LiCl in D_2O. Elemental analyses were performed by ANALEST at the University of Toronto.

$[Li(Et_2O)(thf)LTaMe_3Cl]$, 2

To $[Li_2L(thf)_3]$, **1** (115 mg, 0.175 mmol) dissolved in THF (3 mL) and cooled to −70 °C was added a similarly cooled solution of $TaMe_3Cl_2$ (48.1 mg, 0.162 mmol) in Et_2O (2 mL). The reaction mixture was allowed to warm to room temperature and was stirred for 2 h. Volatiles were removed under reduced pressure. The orange residue was extracted with Et_2O (5 mL), filtered, concentrated to *ca.* 2 mL and cooled to −25 °C overnight. The supernatant was decanted off the crystals that had formed, which were then washed with cold Et_2O (3 × 0.5 mL). Residual solvent was removed by briefly applying vacuum to the yellow crystals of $[Li(Et_2O)(thf)LTaMe_3Cl]$, **2** (63.9 mg, 0.760 mmol, 47%). ^1H NMR (600 MHz, benzene-d_6) δ 7.21 (dd, J = 7.0, 2.1 Hz, 2H), 7.15–7.10 (m, 4H), 5.66–5.62 (m, 2H), 4.04–4.01 (m, 2H), 3.19 (sept, J = 6.9 Hz, 2H), 3.12–3.08 (m, 4H), 3.06 (sept, J = 6.2 Hz, 2H), 1.34 (d, J = 6.9 Hz, 6H), 1.22 (d, J = 6.9 Hz, 6H), 1.20 (d, J = 6.9 Hz, 6H), 1.10 (d, J = 6.8 Hz, 10H) 1.10 (overlapped, 4H), 0.97–0.94 (m, 6H), 0.91 (br, 9H) ^{13}C NMR (151 MHz, benzene-d_6) δ 168.37, 145.38, 142.01, 140.13, 124.84, 123.93, 123.81, 109.94, 86.66, 68.31, 65.99, 28.67, 27.90, 25.30, 24.74, 24.68, 24.54, 24.14, 15.23. We did not observe a resonance attributable to the Ta–Me carbons, presumably due to exchange broadening. ^7Li NMR (233 MHz, benzene-d_6) δ 2.03. Anal. Calcd for $C_{41}H_{65}N_2O_2LiClTa$: C, 58.53; H, 7.79; N, 3.33. Found: C, 58.64; H, 7.60; N, 3.47. Single crystals for XRD were obtained by cooling an Et_2O solution to −25 °C.

$[Li(Et_2O)(thf)LTaMe_4]$, 3(Et_2O)(thf)

$[Li(Et_2O)(thf)LTaMe_3Cl]$, **2** (31.5 mg, 0.0374 mmol), was dissolved in Et_2O (5 mL) and cooled to −35 °C. Methyl lithium (*ca.* 0.16 M in diethylether, 0.22 mL) was added dropwise. The reaction mixture was allowed to warm to room temperature protected from light, and was stirred for 60 min, causing the colour of the solution to lighten. Filtration and removal of volatiles yielded yellow microcrystalline $[Li(Et_2O)(thf)LTaMe_4]$, **3**(Et_2O)(thf) (30.3 mg, 0.0369 mmol, 99%). Anal. Calcd for $C_{42}H_{68}N_2O_2LiTa$: C, 61.45; H, 8.35; N, 3.41. Found: C, 61.72; H, 8.09; N, 3.41. Single crystals of **3**$(thf)_2$ for XRD were obtained by cooling a pentane solution to −25 °C. ^{1}H NMR (500 MHz, benzene-d_6) δ 7.25 (dd, J = 7.2, 1.8 Hz, 2H), 7.19–7.11 (m, 4H), 5.54–5.45 (m, 2H), 4.26–4.18 (m, 2H), 3.28 (sept, J = 7.0 Hz, 2H), 3.15 (br, 4H), 3.07 (sept, J = 6.9 Hz, 2H), 3.04 (q, J = 7.0 Hz, 4H), 1.34 (d, J = 6.9 Hz, 6H), 1.25 (d, J = 6.9 Hz, 6H), 1.23 (d, J = 6.8 Hz, 6H), 1.16 (d, J = 6.8 Hz, 4H), 1.04 (br, 4H), 0.90 (t, J = 7.0 Hz, 6H), 0.89 (br, 12H) ^{13}C NMR (126 MHz, benzene-d_6) δ 164.33, 146.54, 142.45, 140.87, 128.06, 124.31, 123.84, 123.71, 109.26, 89.72, 68.35, 66.01, 28.58, 27.79, 25.19, 24.82, 24.80, 24.60, 24.31, 15.04. We did not observe a resonance attributable to the Ta–Me carbons, presumably due to exchange broadening. ^{7}Li NMR (194 MHz, benzene-d_6) δ 2.26. Anal. Calcd for $C_{42}H_{68}N_2O_2LiTa$: C, 61.45; H, 8.35; N, 3.41. Found: C, 61.72; H, 8.09; N, 3.41. Single crystals of **3**(thf)$_2$ for XRD were obtained by cooling a pentane solution to −25 °C.

[Li$_2$L′(Et$_2$O)$_2$], 5

A hexanes solution of *n*BuLi (1.6 M, 0.29 mL, 0.46 mmol) was added dropwise to a solution of H_2L' (102 mg, 0.223 mmol) in Et_2O cooled to −70 °C using a glove box cold well. The reaction was allowed to warm to room temperature and was stirred for 2 h at which point volatiles were removed *in vacuo*. Pentane (2 mL) was added and the mixture was cooled to −25 °C overnight. The supernatant was decanted off the precipitate which was washed with cold pentane (2 mL) and dried under reduced pressure, leaving fluffy white powder (86 mg, 0.14 mmol, 63%). Due to the highly sensitive nature of this dilithium complex, we could not obtain satisfactory elemental analysis. ^{1}H NMR (300 MHz, benzene-d_6) δ 7.37 (d, J = 7.6 Hz, 4H), 7.22 (dd, J = 8.0, 7.1 Hz, 2H), 6.16 (s, 2H), 3.40 (sept, J = 6.8 Hz, 4H), 2.92 (q, J = 7.1 Hz, 4H), 2.03 (s, 6H), 1.36 (d, J = 6.8 Hz, 12H), 1.29 (d, J = 7.0 Hz, 12H), 0.74 (t, J = 7.1 Hz, 12H). ^{13}C NMR (101 MHz, benzene-d_6) δ 152.74, 144.83, 143.75, 123.79, 121.29, 120.89, 115.05, 66.22, 28.42, 25.27, 25.22, 19.29, 14.10. ^{7}Li NMR (194 MHz, benzene-d_6) δ 0.77. Single crystals for XRD were obtained by cooling a pentane/Et_2O solution to −25 °C.

[LiL′(Et$_2$O)], 6, Method A

[Li$_2$L′(Et$_2$O)$_2$], **5** (0.213 g, 0.353 mmol) was dissolved in THF (8 mL) and cooled to −70 °C using a glove box cold well. A similarly cooled solution of $TaMe_3Cl_2$ (0.104 g, 0.351 mmol) in Et_2O (4 mL) was added dropwise, and the mixture was allowed to warm to room temperature and stirred for 16 h. Volatiles were removed *in vacuo* and pentane (10 mL) was added to the mixture. Insoluble material was filtered off and the filtrate was concentrated and cooled to −25 °C. Crystals formed and were isolated on a fritted funnel; washing with cold pentane (2 × 1 mL) and drying *in vacuo* yielded dark green crystals (0.104 g, 0.194 mmol, 55%). This material was characterized by EPR and XRD, but even multiple recrystallizations did not lead to satisfactory combustion analysis.

[LiL′(Et$_2$O)], 6, Method B

[Li$_2$L’(Et$_2$O)$_2$] (160.8 mg, 0.2607 mmol) was dissolved in toluene (6 mL) and cooled to −25 °C. Under subdued lighting, $AgBF_4$ (50.6 mg, 0.260 mmol) was added as a solid and the mixture was allowed to warm to room temperature with stirring for 2.5 h. At the end of the reaction time, the dark green mixture was filtered through Celite and stripped. Recrystallization of the residue from 5 mL of *ca.* 5% Et_2O in pentane cooled to −25 °C yielded dark green crystals, which were washed with cold pentane and dried *in vacuo* (87.4 mg, 0.163 mmol, 63%). Anal. Calcd for $C_{36}H_{52}N_2OLi$: C, 80.71; H, 9.78; N, 5.22. Found: C, 80.22; H, 9.77; N, 5.05. Single crystals for XRD were obtained by cooling a pentane/Et_2O solution to −25 °C.

[TaLMe$_3$], 8

K_2L: To a solution of H_2L (0.94 g, 2.3 mmol) in toluene (15 mL) cooled to −25 °C was added benzylpotassium (0.61 g, 4.7 mmol)), in one portion. The reaction mixture was allowed to warm to room temperature, and was stirred for 16 h. Pentane (60 mL) was added and the mixture was cooled to −25 °C. The pale green suspension was decanted from any unreacted orange benzylpotassium onto a frit, which left a pale green powder that was then washed with cold toluene (2 × 5 mL) and pentane (2 × 10 mL), and then dried *in vacuo* leaving a pale green pyrophoric powder 0.97 g, 86%.

$TaMe_3Cl_2$ (174 mg, 0.586 mmol) was dissolved in toluene (10 mL) and cooled to −70 °C using a glove box cold well. The vial was removed from the cold well and finely ground K_2L (330 mg, 0.653 mmol) was added as a solid, in portions over five minutes. The reaction turned gradually turned brownish red as it warmed to room temperature. After 5 h, the mixture was filtered through Celite and the toluene was removed under reduced pressure. Recrystallization of the residue from pentane afforded two crops of crystals (143 mg, 0.219 mmol, 37%). ^{1}H NMR (600 MHz, benzene-d_6) δ 7.22–7.21 (m, 6H), 6.52–6.50 (m, 2H), 6.00–5.97 (m, 2H), 3.52 (sept, J = 6.9 Hz, 4H), 1.30 (d, J = 6.9 Hz, 12H), 1.06 (d, J = 6.8 Hz, 12H), 1.03(s, 9H). ^{13}C NMR (151 MHz, C_6D_6) δ 147.80, 146.09, 144.99, 127.61, 124.69, 120.84, 114.77, 83.50, 28.65, 26.29, 24.26. Anal. Calcd for $C_{33}H_{47}N_2Ta$: C, 60.73; H, 7.26; N, 4.29. Found: C, 60.58; H, 7.19; N, 4.21.

DCC insertion product, 9

[TaLMe$_3$] (66 mg, 0.10 mmol) was dissolved in pentane and cooled to −25 °C. A solution of *N*,*N*′-dicyclohexylcarbodiimide (21 mg, 0.10 mmol) in pentane (2 mL) at room temperature was added dropwise. The solution immediately turned cherry red, and was allowed to warm to room temperature with stirring for 16 h. Volatiles were removed under reduced pressure, leaving the insertion product (81 mg, 93%). The analytical sample was washed with pentane. ^{1}H NMR (600 MHz, benzene-d_6) δ 7.31 (d, J = 7.5 Hz, 4H), 7.25 (t, 2H), 6.55–6.51 (m, 2H), 6.06–6.02 (m, 2H), 3.71 (br, 2H), 3.63 (br, 2H), 3.40 (br, 2H), 1.63 (s, 3H), 1.55–1.05 (broad, overlapped, 46 H), 1.03 (s, 6H). ^{13}C NMR (151 MHz, C_6D_6) δ 180.18, 149.05, 146.19, 145.51, 126.75, 125.22 (br), 124.03 (br), 120.40, 115.88, 75.25, 65.92, 59.37, 35.40, 32.81, 28.61, 28.10, 26.51, 25.81, 24.88, 24.30, 15.12. Anal. Calcd for $C_{46}H_{69}N_4Ta$: C, 64.32; H, 8.10; N, 6.52. Found: C, 64.23; H, 8.06; N, 6.69. Single crystals for XRD were obtained by allowing a pentane solution to slowly evaporate at room temperature.

$MesN_3$ insertion product, 10

Pentane was added to [$TaLMe_3$] (51.5 mg, 0.0789 mmol) and the brown mixture was cooled to −25 °C. A solution of mesityl azide (13.4 mg, 0.0831 mmol) in pentane (0.5 mL) was added dropwise. The mixture was allowed to warm to room temperature and was stirred for 2 h, causing a precipitate to form. Volatiles were removed under reduced pressure and the residue was washed with cold pentane (3 × 0.5 mL). Drying *in vacuo* left orange powder (40.7 mg, 0.0500 mmol, 63%). The analytical sample was recrystallized from toluene. ^{1}H NMR (600 MHz, benzene-d_6) δ 7.24–7.21 (m, 6H), 6.70 (s, 2H), 6.67–6.61 (m, 2H), 6.29–6.24 (m, 2H), 3.35 (sept, J = 6.9 Hz, 4H), 2.53 (s, 3H), 2.09 (s, 6H), 2.06 (s, 3H), 1.10 (d, J = 6.8 Hz, 12H), 1.09 (d, J = 6.8 Hz, 12H), 0.67 (s, 6H). ^{13}C NMR (151 MHz, benzene-d_6) δ 147.94, 145.98, 145.46, 145.25, 135.56, 129.61, 129.40, 127.24, 124.78, 120.53, 114.94, 63.06, 35.02, 28.24, 25.38, 24.83, 20.84, 18.58. Anal. Calcd for $C_{42}H_{58}N_5Ta$: C, 61.98; H, 7.18; N, 8.60. Found: C, 61.76; H, 6.98; N, 8.76. Single crystals for XRD were obtained by cooling an Et_2O solution to −25 °C.

[$TaLMe_2$]$_2$, 11

A pyrex reaction vessel was charged with a solution of [$TaLMe_3$] (46.7 mg, 0.0716 mmol) in toluene (30 mL) and was sealed with a Teflon screw cap. The bomb was irradiated with a 450 W Ace Glass medium-pressure mercury lamp inside a photochemical reaction cabinet for 3 h. After removal of volatile components, the residue was extracted with pentane and filtered through Celite. Concentration of the filtrate and cooling to −25 °C caused formation of red-orange crystals. The supernatant was decanted and the crystals were washed with cold pentane (3 × 1 mL). Drying *in vacuo* yielded analytically pure [$TaLMe_2$]$_2$·(pentane)$_{2/3}$ (9.0 mg, 0.0068 mmol, 19%). ^{1}H NMR (500 MHz, benzene-d_6) δ 7.21–7.18 (m, 8H), 7.13 (dd, J = 8.5, 6.7 Hz, 4H), 6.30–6.25 (m, 4H), 5.81–5.75 (m, 4H), 3.66 (sept, J = 6.8 Hz, 8H), 1.19 (d, J = 6.9 Hz, 24H), 1.03 (d, J = 6.7 Hz, 24H), 0.08 (s, 12H). ^{13}C NMR (126 MHz, C_6D_6) δ 150.06, 145.41, 145.21, 127.51, 124.78, 121.31, 114.73, 49.22, 28.00, 26.24, 24.73. Anal. Calcd for $C_{64}H_{88}N_4Ta_2(C_5H_{12})_{2/3}$: C, 61.11; H, 7.31; N, 4.23. Found: C, 61.17; H, 7.29; N, 3.96. Note: the ratio of **11** to pentane was determined by integration of the ^{1}H NMR spectrum. Single crystals for XRD were obtained by cooling a pentane solution to −25 °C.

Acknowledgements

We thank NSERC of Canada for funding. T. J. thanks the government of Ontario for an Ontario Graduate Scholarship and the University of Toronto a QEII-GSST scholarship. We thank Digital Specialty Chemicals for providing $TaCl_5$ and P^tBu_3. Thanks to Dr Timothy Burrow for assistance with EPR. We also acknowledge the Canadian Foundation for Innovation Project #19119, and the Ontario Research Fund for funding the CSICOMP NMR lab at the University of Toronto enabling the purchase of several new spectrometers.

References

1 G. L. Juvinall, *J. Am. Chem. Soc.*, 1964, **86**, 4202–4203.
2 R. R. Schrock and P. Meakin, *J. Am. Chem. Soc.*, 1974, **96**, 5288–5290.
3 R. R. Schrock, *J. Organomet. Chem.*, 1976, **122**, 209–225.
4 R. R. Schrock and P. R. Sharp, *J. Am. Chem. Soc.*, 1978, **100**, 2389–2399.
5 M. D. Fryzuk, S. A. Johnson and S. J. Rettig, *J. Am. Chem. Soc.*, 1998, **120**, 11024–11025.
6 P. Garcia, Y. Y. Lau, M. R. Perry and L. L. Schafer, *Angew. Chem., Int. Ed.*, 2013, **52**, 9144–9148.
7 Y. Chen, E. Callens, E. Abou-Hamad, N. Merle, A. J. P. White, M. Taoufik, C. Copéret, E. Le Roux and J. Basset, *Angew. Chem., Int. Ed.*, 2012, **51**, 11886–11889.
8 Y. Chen, E. Abou-hamad, A. Hamieh, B. Hamzaoui, L. Emsley and J. Basset, *J. Am. Chem. Soc.*, 2015, **137**, 588–591.
9 M. D. Fryzuk, S. A. Johnson, B. O. Patrick, A. Albinati, S. A. Mason and T. F. Koetzle, *J. Am. Chem. Soc.*, 2001, **123**, 3960–3973.
10 M. D. Fryzuk, B. A. MacKay, S. A. Johnson and B. O. Patrick, *Angew. Chem., Int. Ed.*, 2002, **41**, 3709–3712.
11 M. D. Fryzuk, B. A. MacKay and B. O. Patrick, *J. Am. Chem. Soc.*, 2003, **125**, 3234–3235.
12 M. P. Shaver, S. A. Johnson and M. D. Fryzuk, *Can. J. Chem.*, 2005, **83**, 652–660.
13 B. A. MacKay, R. F. Munha and M. D. Fryzuk, *J. Am. Chem. Soc.*, 2006, **128**, 9472–9483.
14 B. A. MacKay, B. O. Patrick and M. D. Fryzuk, *Organometallics*, 2005, **24**, 3836–3841.
15 J. Ballmann, F. Pick, L. Castro, M. D. Fryzuk and L. Maron, *Organometallics*, 2012, **31**, 8516–8524.
16 J. Ballmann, F. Pick, L. Castro, M. D. Fryzuk and L. Maron, *Inorg. Chem.*, 2013, **52**, 1685–1687.
17 K. D. J. Parker, D. Nied and M. D. Fryzuk, *Organometallics*, 2015, **34**, 3546–3558.
18 J. Ballmann, A. Yeo, B. A. MacKay, S. v. Rijt, B. O. Patrick and M. D. Fryzuk, *Chem. Commun.*, 2010, **46**, 8794–8796.
19 J. Ballmann, A. Yeo, B. O. Patrick and M. D. Fryzuk, *Angew. Chem., Int. Ed.*, 2011, **50**, 507–510.
20 M. D. Fryzuk, S. A. Johnson and S. J. Rettig, *Organometallics*, 1999, **18**, 4059–4067.
21 M. D. Fryzuk, S. A. Johnson and S. J. Rettig, *Organometallics*, 2000, **19**, 3931–3941.
22 M. D. Fryzuk, S. A. Johnson and S. J. Rettig, *J. Am. Chem. Soc.*, 2001, **123**, 1602–1612.
23 A. I. Nguyen, K. J. Blackmore, S. M. Carter, R. A. Zarkesh and A. F. Heyduk, *J. Am. Chem. Soc.*, 2009, **131**, 3307–3316.
24 A. F. Heyduk, R. A. Zarkesh and A. I. Nguyen, *Inorg. Chem.*, 2011, **50**, 9849–9863.

25 R. F. Munhá, R. A. Zarkesh and A. F. Heyduk, *Inorg. Chem.*, 2013, **52**, 11244–11255.

26 R. R. Schrock, J. Lee, L. Liang and W. M. Davis, *Inorg. Chim. Acta*, 1998, **270**, 353–362.

27 J. P. Araujo, D. K. Wicht, P. J. Bonitatebus and R. R. Schrock, *Organometallics*, 2001, **20**, 5682–5689.

28 L. P. H. Lopez, R. R. Schrock and P. J. Bonitatebus Jr., *Inorg. Chim. Acta*, 2006, **359**, 4730–4740.

29 J. S. Freundlich, R. R. Schrock and W. M. Davis, *Organometallics*, 1996, **15**, 2777–2783.

30 J. S. Freundlich, R. R. Schrock and W. M. Davis, *J. Am. Chem. Soc.*, 1996, **118**, 3643–3655.

31 I. A. Tonks and J. E. Bercaw, *Inorg. Chem.*, 2010, **49**, 4648–4656.

32 M. E. G. Skinner, D. A. Cowhig and P. Mountford, *Chem. Commun.*, 2000, 1167–1168.

33 M. E. G. Skinner, T. Toupance, D. A. Cowhig, B. R. Tyrrell and P. Mountford, *Organometallics*, 2005, **24**, 5586–5603.

34 F. Guérin, D. H. McConville and J. J. Vittal, *Organometallics*, 1995, **14**, 3154–3156.

35 F. Guérin, D. H. McConville, J. J. Vittal and G. A. P. Yap, *Organometallics*, 1998, **17**, 1290–1296.

36 L. P. Spencer, C. Beddie, M. B. Hall and M. D. Fryzuk, *J. Am. Chem. Soc.*, 2006, **128**, 12531–12543.

37 C. D. Carmichael, M. P. Shaver and M. D. Fryzuk, *Can. J. Chem.*, 2006, **84**, 1667–1678.

38 R. Fandos, J. Fernández-Gallardo, A. Otero, A. Rodríguez and M. J. Ruiz, *Organometallics*, 2011, **30**, 1551–1557.

39 P. Bazinet, G. P. A. Yap and D. S. Richeson, *Organometallics*, 2001, **20**, 4129–4131.

40 N. Lavoie, S. I. Gorelsky, Z. Liu, T. J. Burchell, G. P. A. Yap and D. S. Richeson, *Inorg. Chem.*, 2010, **49**, 5231–5240.

41 J. M. Decams, S. Daniele, L. Hubert-Pfalzgraf, J. Vaissermann and S. Lecocq, *Polyhedron*, 2001, **20**, 2405–2414.

42 S. Feng, G. R. Roof and E. Y. X. Chen, *Organometallics*, 2002, **21**, 832–839.

43 T. Chen, C. Xu, T. H. Baum, G. T. Stauf, J. F. Roeder, A. G. DiPasquale and A. L. Rheingold, *Chem. Mater.*, 2010, **22**, 27–35.

44 K. Mashima, Y. Matsuo and K. Tani, *Chem. Lett.*, 1997, **26**, 767–768.

45 K. Mashima, Y. Matsuo and K. Tani, *Organometallics*, 1999, **18**, 1471–1481.

46 J. Sánchez-Nieves, P. Royo, M. A. Pellinghelli and A. Tiripicchio, *Organometallics*, 2000, **19**, 3161–3169.

47 H. Kawaguchi, Y. Yamamoto, K. Asaoka and K. Tatsumi, *Organometallics*, 1998, **17**, 4380–4386.

48 H. Tsurugi, T. Ohno, T. Kanayama, R. A. Arteaga-Müller and K. Mashima, *Organometallics*, 2009, **28**, 1950–1960.

49 H. Tsurugi, T. Saito, H. Tanahashi, J. Arnold and K. Mashima, *J. Am. Chem. Soc.*, 2011, **133**, 18673–18683.

50 K. Aoyagi, P. K. Gantzel and T. D. Tilley, *Polyhedron*, 1996, **15**, 4299–4302.

51 G. Jimenez Pindado, M. Thornton-Pett and M. Bochmann, *J. Chem. Soc., Dalton Trans.*, 1998, 393–400.

52 A. Grundmann, M. B. Sárosi, P. Lönnecke, R. Frank and E. Hey-Hawkins, *Eur. J. Inorg. Chem.*, 2013, 3137–3140.

53 A. Grundmann, M. B. Sárosi, P. Lönnecke and E. Hey-Hawkins, *Eur. J. Inorg. Chem.*, 2014, 2997–3001.

54 V. Tabernero, T. Cuenca, M. E. G. Mosquera and C. R. de Arellano, *Polyhedron*, 2009, **28**, 2545–2554.

55 T. Janes, J. M. Rawson and D. Song, *Dalton Trans.*, 2013, **42**, 10640–10648.

56 R. H. Crabtree, in *The Organometallic Chemistry of the Transition Metals*, Wiley, Hoboken, New Jersey, 5th edn, 2009, pp. 122–152.

57 T. Wenderski, K. M. Light, D. Ogrin, S. G. Bott and C. J. Harlan, *Tetrahedron Lett.*, 2004, **45**, 6851–6853.

58 G. W. A. Fowles, D. A. Rice and J. D. Wilkins, *J. Chem. Soc., Dalton Trans.*, 1973, 961–965.

59 J. D. Wilkins, *J. Organomet. Chem.*, 1974, **80**, 349–355.

60 R. A. Zarkesh and A. F. Heyduk, *Organometallics*, 2011, **30**, 4890–4898.

61 W. J. Evans, J. R. Walensky, J. W. Ziller and A. L. Rheingold, *Organometallics*, 2009, **28**, 3350–3357.

62 B. Liu and D. Cui, *Dalton Trans.*, 2009, 550–556.

63 W. J. Evans, T. J. Mueller and J. W. Ziller, *J. Am. Chem. Soc.*, 2009, **131**, 2678–2686.

64 E. M. Matson, W. P. Forrest, P. E. Fanwick and S. C. Bart, *Organometallics*, 2013, **32**, 1484–1492.

65 S. J. Kraft, P. E. Fanwick and S. C. Bart, *Organometallics*, 2013, **32**, 3279–3285.

66 M. Schlosser and J. Hartmann, *Angew. Chem., Int. Ed. Engl.*, 1973, **12**, 508–509.

67 S. Wiese, M. J. B. Aguila, E. Kogut and T. H. Warren, *Organometallics*, 2013, **32**, 2300–2308.